Cellular Physiology and Biochemistry
Cell Physiol Biochem 2018;51:1461-1479
DOI: 10.1159/000495594
Published online: 28 November 2018
Accepted: 20 November 2018

Original Paper

Different PDGF Receptor Dimers Drive Distinct Migration Modes of the Mouse Skin Fibroblast

Kohta Yamada[a,b] Takeru Hamashima[a] Yoko Ishii[a] Seiji Yamamoto[a] Noriko Okuno[a] Naofumi Yoshida[a] Moe Yamada[a] Ting Ting Huang[a] Norifumi Shioda[c] Kei Tomihara[b] Toshihiko Fujimori[d] Hisashi Mori[e] Kohji Fukunaga[f] Makoto Noguchi[b] Masakiyo Sasahara[a]

[a]Department of Pathology, Graduate School of Medicine and Pharmaceutical Sciences, University of Toyama, Toyama, [b]Department of Oral and Maxillofacial Surgery, Graduate School of Medicine and Pharmaceutical Sciences, University of Toyama, Toyama, [c]Department of Biofunctional Analysis Laboratory of Molecular Biology, Gifu Pharmaceutical University, Gifu, [d]Division of Embryology, National Institute for Basic Biology, Okazaki, [e]Department of Molecular Neuroscience, Graduate School of Medicine and Pharmaceutical Sciences, University of Toyama, Toyama, [f]Department of Pharmacology, Graduate School of Pharmaceutical Sciences, Tohoku University, Sendai, Japan

Key Words
Platelet derived growth factor • Receptor • Chemotaxis • Fibroblast • Directionality • Signaling • Cytoskeleton

Abstract
Background/Aims: The migration of mesenchymal cells is a fundamental cellular process that has been implicated in many pathophysiological conditions and is induced by chemoattractants such as platelet-derived growth factors (PDGFs). However, the regulatory mechanisms shaping this migration remain to be elucidated. ***Methods:*** Here, we prepared mouse skin fibroblasts inactivated for different PDGF receptor genes and systematically measured their chemotactic responses within a gradient of different chemoattractants. ***Results:*** We found that PDGFRαβ and PDGFRββ dimers were strong inducers of random and directionally-persistent migration, respectively, that was sustained for up to 24 h. MAPK and PI3K were necessary to mediate random and directional migration, respectively. Directional migration was accompanied by abundant ventral stress fiber formation and consistent cell shape with less frequent formation of branch-like processes. ***Conclusion:*** This is the first systematic study that characterized the chemotaxis mediated by three-different types of PDGFR dimers in mesenchymal cell migration. Our data demonstrate that PDGFR dimer formation is the critical step to determine the specific mode of fibroblast chemotaxis, while the accompanying cytoskeletal remodeling might contribute to migration persistence.

Seiji Yamamoto, Ph.D
and Yoko Ishii, M.D, Ph.D

Department of Pathology, Graduate School of Medicine and Pharmaceutical Sciences
University of Toyama, Toyama 930-0194 (Japan)
E-Mail seiyama@med.u-toyama.ac.jp, seiyama.flyfishing@gmail.com; yishii@ems.u-toyama.ac.jp

Introduction

Migration is a fundamental cell behavior implicated in many physiological and pathological phenomena, including organogenesis, wound healing, and cancer metastasis. To control motility in accordance with various physiological and pathological conditions, cell movements are regulated by different mechanisms. These include chemotaxis, haptotaxis, electrotaxis, and durotaxis [1]. Chemotaxis is a relatively well-understood form of cell motility motivated by soluble, extracellular cues, and is mediated by a variety of signaling pathways [2, 3]. Whereas amoeboid cells such as leukocytes exhibit robustly polarized movement in response to these cues, mesenchymal cells such as fibroblasts migrate slowly and are believed to exhibit only weakly polarized migration [4].

Mesenchymal cells crawl by balancing actin polymerization and integrin-mediated adhesion dynamics at their leading edges, which often merge as multiple competing protrusions (lamellipodia and filopodia) radiating in different directions to drive cell migration [1, 5, 6]. Accumulated data have indicated that a broad network of downstream signaling molecules of PI3-Akt and Rho GTPase, regulates this cytoskeletal remodeling and the accompanying changes in cell shape and has additionally been hypothesized to define the mode of cell movement, such as random versus directionally-persistent migration, as well as migration velocity [7-12]. On the other hand, the other studies have indicated that neither PI3-Akt nor Rho GTPase is absolutely required for chemotaxis [13, 14]. While the modulation of these signaling intermediates affects cell morphology and migration speed, the ability to sense and respond to a chemoattractant cue is not grossly affected [15, 16]. Furthermore, Ras-PI3 Kinase-Rac GTPase axis was involved in the motility of mouse embryonic fibroblasts induced by epidermal growth factor, but not in that induced by platelet-derived growth factor (PDGF) [17]. Thus, the basic mechanisms of cell motility, such like asymmetric morphology with defined leading and trailing edges, and polarized intracellular signalling, are well understood; however, it still remains unknown the mechanism by which soluble extracellular cues are transduced into these intrinsic signaling networks and how they define the mode of cell motility is poorly understood in mesenchymal cells [3, 4].

PDGFs are potent mitogens and chemoattractants for mesenchymal cells such as invading fibroblasts in skin wounds [18, 19]. Ligands that can bind to PDGFRαα with high affinity are PDGF-AA, -BB, and -CC, while PDGF-BB and -DD have high affinity for PDGFRββ [20, 21]. PDGF-AB and -CC are abundant in platelets and preferentially activate PDGFRαβ in cells that express both PDGFR subunits [22-25]. PDGFRα and PDGFRβ subunits mediate similar mitogenic effects but different migratory responses. PDGFRβ is a common mediator of cell migration in various mesenchymal cells, including skin fibroblasts, smooth muscle cells, and NIH3T3 fibroblasts [26-28]. In contrast, PDGFRα either positively or negatively regulates the migration of these cells depending on their cell type [26-29]. Therefore, the roles of different PDGF ligands in cell migration are not well conceptualized and could be due to a lack of knowledge on the functional significance of the three types of PDGFR dimers.

In the present study, we sought to clarify the regulatory mechanism of PDGF-induced chemotaxis in primary cultured skin fibroblasts in order to increase our understanding of pathophysiological phenomena in which fibroblast or mesenchymal cell recruitments are crucial components. To this end, we prepared mouse skin fibroblasts inactivated for different *Pdgfr* genes and systematically measured their chemotactic responses in a microfluid chamber, which establishes a stable gradient of chemoattractants. We found, for the first time, that different PDGFR dimers independently modify velocity and directionality of cell migration, and that PDGFRαβ and PDGFRββ dimers mediate random and directional migrations toward soluble cues, respectively, with different signal dependencies. PDGFRββ mediated directionally-persistent migration, which was accompanied by cytoskeletal remodeling such as abundant ventral stress fiber formation, for up to 24 h. Our data indicates that PDGFR dimer formation is the critical step to determine the specific mode of fibroblast chemotaxis, while the accompanying cytoskeletal remodeling might contribute to migration persistence.

Materials and Methods

Ethics

All animal procedures were conducted in accordance with guidelines laid out by the Institutional Animal Care and Use Committee at the University of Toyama (University of Toyama, Sugitani, Toyama City, Japan). All study protocols were approved by the Ethics Committee of the University of Toyama before the study began.

Generation of Transgenic Mice and Harvest of Primary Fibroblasts

Mice harbouring a *Pdgfra* gene in which exons 4–5 were flanked by *loxP* sequences (*Pdgfra*$^{flox/flox}$) were generated as previously described [30]. Genotyping was performed by PCR using the following primers: 5'-ATGCCAAACTCTGCCTGATTGA-3' and 5'-CTCACGGAACCCCCACAAC-3'. *Pdgfrb*$^{flox/flox}$ mice, in which exons 4–7 of *Pdgfrb* were flanked by loxP sequences, were generated as previously described [26]. Genotyping was performed by PCR using the following primers: 5'-AGGACAACCGTACCTTGGGTGACT-3' and 5'-CAGTTCTGACACGTACCGGGTCTC-3'. *Pdgfra*$^{flox/flox}$ and *Pdgfrb*$^{flox/flox}$ mice were bred with transgenic mice that systemically express 4-OH-tamoxifen (TM)-inducible Cre recombinase (CAGGCre-ER$^{TM+/-}$; Jackson, Bar Harbor, ME, USA) [31].

Skin was harvested from the resulting pups at postnatal days 1 to 3 under deep anesthesia (50 mg pentobarbital per kg of body weight, intraperitoneal injection). After collagenase treatment, dissociated skin fibroblasts were cultured in D-MEM (Nacalai Tesque, Kyoto, Japan) containing 10 % FBS (NICHIREI BIOSCIENCES INC, Tokyo, Japan) as previously described [30]. Isolated *Pdgfra*$^{flox/flox}$*; Cre-ER*$^{TM+/-}$*, Pdgfrb*$^{flox/flox}$*; Cre-ER*$^{TM+/-}$*, Pdgfra*$^{flox/flox}$*; Pdgfrb*$^{flox/flox}$*; Cre-ER*$^{TM+/-}$ and *Pdgfra*$^{flox/flox}$*; Pdgfrb*$^{flox/flox}$*; Cre-ER*$^{TM-/-}$ fibroblasts were treated with 1 μM 4-hydroxytamoxifen (4-OHT) (Sigma-Aldrich, Louis, MO) for 48 h in order to obtain fibroblasts with inactivation of *Pdgfra, Pdgfrb* and both of the two genes (corresponding to α-KO, β-KO, αβ-KO, respectively), and control Flox fibroblasts, respectively (Supplementary Fig. 1 - for all supplemental material see www.karger.com/ 10.1159/000495594).

Chemotaxis Assay

Chemotaxis was analyzed using the Millicell μ-Migration Assay Kit (Millipore, Billerica, MA) according to manufacturer's instructions. This system enables the generation of a stable and linear concentration gradient of soluble chemoattractant through diffusion, which can be maintained in a μ-Migration chamber slide for 48 hours. Briefly, the μ-Migration chamber slide was coated with collagen type I (BD biosciences, San Jose, CA) before use. 4-OHT-treated fibroblasts of varying genotypes were seeded into the observation chamber at a concentration of $3x10^6$ cells/ml then incubated at 37 °C with 5% CO_2 and a humid atmosphere for 3-6 h. After washing out the non-adherent cells, fibroblasts were serum-starved overnight in D-MEM containing 0.1% BSA. One reservoir was filled with serum-free D-MEM while the other was filled with D-MEM containing chemoattractants in order to construct a gradient of chemoattractant between the two reservoirs. Images of the μ-Migration chamber slides were taken every 30 min for up to 24 h using an inverted phase contrast microscope (KEYENCE BZ-9000, Osaka, Japan). Using these time-lapse images, chemotaxis was quantified as previously described [32]. Briefly, cells were tracked using the manual tracking plugin for ImageJ (NIH, Bethesda, MD) to retrieve the coordinates (*x, y*) and migration distance of a single cell. The migration tracks were plotted after setting the starting point for each cell at x = 0, and y = 0, using the ImageJ chemotaxis and migration tool plugin. Black and red tracks indicate individual cells with net migration toward (= plus) and away from (= minus) the chemoattractant cue, respectively. The directionality of the chemotactic response was quantified by calculating the yFMI, where the net change in the *y* direction of a given track is divided by the total accumulated path length traveled to that endpoint. The chemotactic index a. u. (unit of yFMI) was determined for the tracked cells with the Chemotaxis and Migration Tool plugin of ImageJ. yFMI quantifies the chemotactic response of cells by dividing the net Δy value of a given track by total accumulated distance traveled to that endpoint. The value for yFMI was calculated as follows:

$$yFMI = \text{net change in y direction/total path length} = \Sigma\Delta y/\Sigma\,(\Delta x^2 + \Delta y^2)^{1/2}$$

The sums for individual cells in above equation were carried out for coordinates (x, y) determined every 30 min over the observation period of 24 h [32]. Experiments were replicated a minimum of three

times, and the representative results are presented. PDGF-AB and PDGF-BB were purchased from PeproTech Inc. (Rocky Hill, NJ). The Ras inhibitor FTA was obtained from Santa Cruz Biotechnology, Inc. (Santa Cruz, CA). The MEK inhibitor PD98059 and PI3K inhibitor LY294002 were purchased from Millipore.

Wound Scratch Assay

The wound scratch assay was performed as reported previously [26]. Briefly, confluent cultures of α-KO, β-KO, αβ-KO, and Flox fibroblasts were serum-starved for 24 h in D-MEM, scratched with a 1 ml plastic pipette tip, and then washed twice with PBS to remove the floating cell debris. The cells were then cultured in D-MEM supplemented with 10 % FBS. After 6, 12, 18, and, 48 h, the cells were viewed with an inverted phase contrast microscope (KEYENCE BZ-9000, Osaka, Japan) and photographed to monitor scratched wound closure.

Western Blotting

α-KO, β-KO, αβ-KO, and Flox fibroblasts were serum-starved for 24 h and then treated with FBS or PDGF-BB as indicated elsewhere. Sample preparation and western blotting procedures were followed as described elsewhere [33, 34]. After transferring, the membranes were blocked for 1 h at 20 °C in a buffer containing 50 mM Tris, 150 mM NaCl, 0.1 % Tween 20, and 5 % nonfat dry milk. The membranes were then probed with the following antibodies: rabbit anti-PDGFRα (1:1000, Santa Cruz Biotechnology, Inc.), rabbit anti-PDGFRβ (1:500, Upstate/Millipore), mouse anti-Akt (1:1000. Santa Cruz Biotechnology, Inc.), rabbit anti-phospho-Akt (1:500, Cell Signaling Technology, Inc., Beverly, MA), rabbit anti-Erk (1:1000, Cell Signaling Technology, Inc.), rabbit anti-phospho-Erk (1:1000, Cell Signaling Technology, Inc.), and mouse anti-GAPDH (1:5000, Chemicon/Millipore, Billerica, MA). Immunoreactive bands were detected using enhanced chemiluminescence reagents (Amersham Biosciences, Little Chalfont, UK) according to the manufacturer's instructions. For immunoprecipitation, extracts containing 200 μg of protein were incubated with 5 μg of anti-PDGFRβ and 30 μL of protein A-Sepharose CL-4B suspension (50 %, v/v), made up to a total volume of 300 μL with cell lysis buffer. This mixture was then incubated for 4 h at 4 °C. Immunoprecipitate was lysed with cell lysis buffer and used for western blotting analysis with an anti-PDGFRα (1:1000) or anti-PDGFRβ (1:500) antibody.

Immunofluorescent Staining

Cultured cells were fixed in 4 % paraformaldehyde on ice for 5 min and then changed to PBS. Specimens were permeabilized in a 0.3 % Triton X-100/PBS solution for 30 min and then blocked for 30 min using the Protein-Block Kit (Dako, Glostrup, Denmark). Blocked specimens were incubated with primary antibodies diluted in Dako diluents (Glostrup, Denmark) for two overnights at 4 °C. The following primary antibodies were used: rabbit anti-phospho-PDGFRβ (1:50, Santa Cruz Biotechnology, Inc.) and mouse anti-vinculin (1:100, Sigma-Aldrich). The secondary antibodies used were Alexa-Fluor488, Alexa-Fluor568, or Alexa-Fluor633 (Invitrogen/Life Technologies Corporation, Carlsbad, CA), at dilutions of 1:500. For F-actin staining, Alexa-Fluor 670-conjugated phalloidin (Cytoskeleton Inc., Denver, CO) was used. Nuclei were stained with Hoechst 33258 (Nacalai Tesque, Kyoto, Japan). As previously described [35, 36], imaging was performed on a LSM780 confocal system (Carl Zeiss, Oberkochen, Germany), a Leica TCS SP5 confocal system (Leica Microsystems, Wetzlar, Germany), and a KEYENCE BZ-9000 fluorescent microscope (KEYENCE, Osaka, Japan).

Statistical Analysis

Quantitative data were expressed as means ± SEM. Two-way ANOVA followed by Tukey's method was used for statistical analysis, with p value less than 0.05 considered significant.

Results

Generation of PDGFRα, PDGFRβ, or PDGFRαβ-deficient fibroblasts

The chemotactic responses mediated by different PDGFR dimers were examined using primary cultures of mouse skin fibroblasts in which either or both of the *Pdgfr* genes were inactivated by tamoxifen (TM)-inducible Cre recombinase *in vitro*. In western blot analyses, PDGFRα and PDGFRβ proteins were expressed in TM-treated control fibroblasts that carried *Pdgfra* and *Pdgfrb* genes flanked by two loxP sequences (flox alleles) but no *CAGG-Cre* transgene (Flox fibroblasts; Supplementary Fig. 1). In contrast, PDGFRα, PDGFRβ, or both together were efficiently depleted after TM treatment of cells harboring flox alleles of the corresponding gene(s) in addition to the *CAGG-Cre* transgene. These cells were termed α-KO, β-KO, and αβ-KO fibroblasts, respectively (Supplementary Fig. 1). In α-KO and β-KO fibroblasts, the expression levels of PDGFR from wild-type alleles were comparable to those in Flox fibroblasts. Therefore, the effects of gene inactivation were specific to the flox allele. This also implied that, for example, PDGF-BB stimulation could induce PDGFRαα and PDGFRββ homodimers in β-KO and α-KO fibroblasts, respectively.

PDGFRββ promotes directional migration in Pdgfra-invalidated fibroblasts

Chemotaxis was analyzed by time-lapse, video-monitored trajectories of cultured fibroblasts observed for up to 24 h. Representative video stills of cultured fibroblasts in migration chambers are shown in Supplementary Fig. 2. At first, the chemotaxis mediated by each PDGFR homodimer was characterized in α-KO and β-KO fibroblasts, using αβ-KO fibroblasts as controls. The trajectories of α-KO fibroblasts tended to run parallel to the gradient, heading toward the increasing concentration of FBS and resulting in a positive net migration (black lines, Fig. 1A) in an FBS gradient (30–0%) generated between basal medium (D-MEM) supplemented with or without 30% FBS. This indicated directionally-persistent migration toward soluble chemoattractants with less frequent turning. Intriguingly, the trajectories of β-KO fibroblasts were very different, appearing as a mix of both plus and minus net migrations (black and red lines, Fig. 1B) with complex configurations corresponding to frequent turning behaviors. Similar to β-KO fibroblasts, αβ-KO fibroblasts showed randomly-arranged trajectories with complex configurations comprised of both plus and minus net migrations which were more widely spread than in the β-KO fibroblasts (Fig. 1C). Migration distances were estimated from the total path length and were found to be similar among the three fibroblast genotypes when cultured in an FBS gradient (Fig. 1D, distance, 430.33 ± 27.73 μm in α-KO, 340.54 ± 19.44 μm in β-KO, and 451.12 ± 38.21 μm in αβ-KO). The directionality of migration (yFMI: y forward migration index), estimated as previously reported [32], was much higher in α-KO than in other fibroblasts when cultured in an FBS gradient (Fig. 1E, yFMI, a.u., 0.60 ± 0.030 in α-KO, −0.0030 ± 0.065 in β-KO, and 0.093 ± 0.072 in αβ-KO, $p < 0.01$ for α-KO vs. β-KO and α-KO vs. αβ-KO).

In a PDGF-BB gradient of 5–0 nM, the trajectories of α-KO fibroblasts showed directionally-persistent migration toward more concentrated levels of PDGF-BB and exhibited less frequent turning (Fig. 1F). Under the same experimental conditions, the trajectories of β-KO and αβ-KO fibroblasts were of complex configurations that indicated frequent turning behavior (Fig. 1G and 1H). Net migration was slightly shifted toward the plus in β-KO fibroblasts (Fig. 1G) and was of proportionally mixed plus and minus routes in αβ-KO fibroblasts (Fig. 1H). It is of note that the movements of αβ-KO fibroblasts in the PDGF-BB gradient corresponded to spontaneous cell movements independent of extracellular chemoattractant cues (Fig. 1H). Migration distance in the PDGF-BB gradient was significantly larger for the α-KO and β-KO fibroblasts than for the αβ-KO fibroblasts (Fig. 1I, distance, 694.59 ± 36.68 μm in α-KO, 720.87 ± 35.45 μm in β-KO, and 543.13 ± 27.56 μm in αβ-KO, $p < 0.01$ for α-KO vs. αβ-KO and β-KO vs. αβ-KO). The yFMI of these cells was highest for the α-KO fibroblasts (Fig. 1J, yFMI, a.u., 0.67 ± 0.03 in α-KO, 0.24 ± 0.05 in β-KO, −0.07 ± 0.05 in αβ-KO, $p < 0.01$ in α-KO vs. β-KO and α-KO vs. αβ-KO), followed by the β-KO and then the αβ-KO.

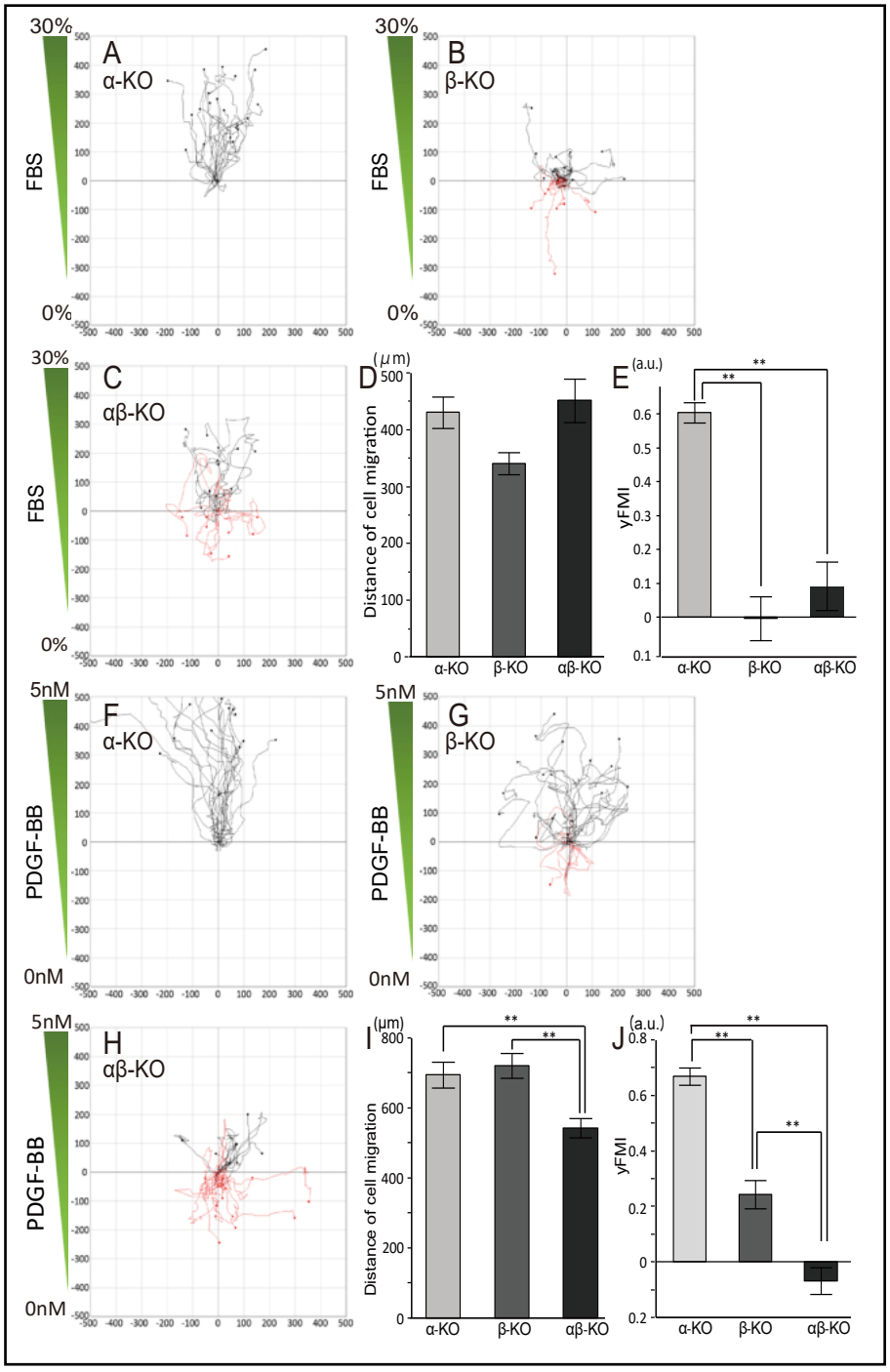

Fig. 1. PDGFR homodimers mediate the directional migration of fibroblasts. (A-C) Trajectories of α-KO (A), β-KO (B), and αβ-KO (C) fibroblasts cultured in the presence of an FBS gradient from 30-0%. (D and E) Distance of cell migration (D) and yFMI (E) were compared over 24 h between the different fibroblast genotypes in response to an FBS gradient (30–0%). (F–H) Trajectories of α-KO (F), β-KO (G), and αβ-KO (H) fibroblasts cultured in the presence of a PDGF-BB gradient from 5-0 nM. (I and J) Distances of cell migration (I) and yFMI (J) were compared over 24 h between the different fibroblast genotypes in response to a PDGF-BB gradient (5-0 nM). Black and red trajectory lines show, respectively, plus and minus net migration along the chemoattractant gradient. Green triangles indicate the chemoattractant gradient. Twenty cells were randomly selected from each experiment for preparing trajectories. Experiments were replicated a minimum of three times, and the representative results are presented. All error bars indicate the mean ± SEM. (** = p<0.01).

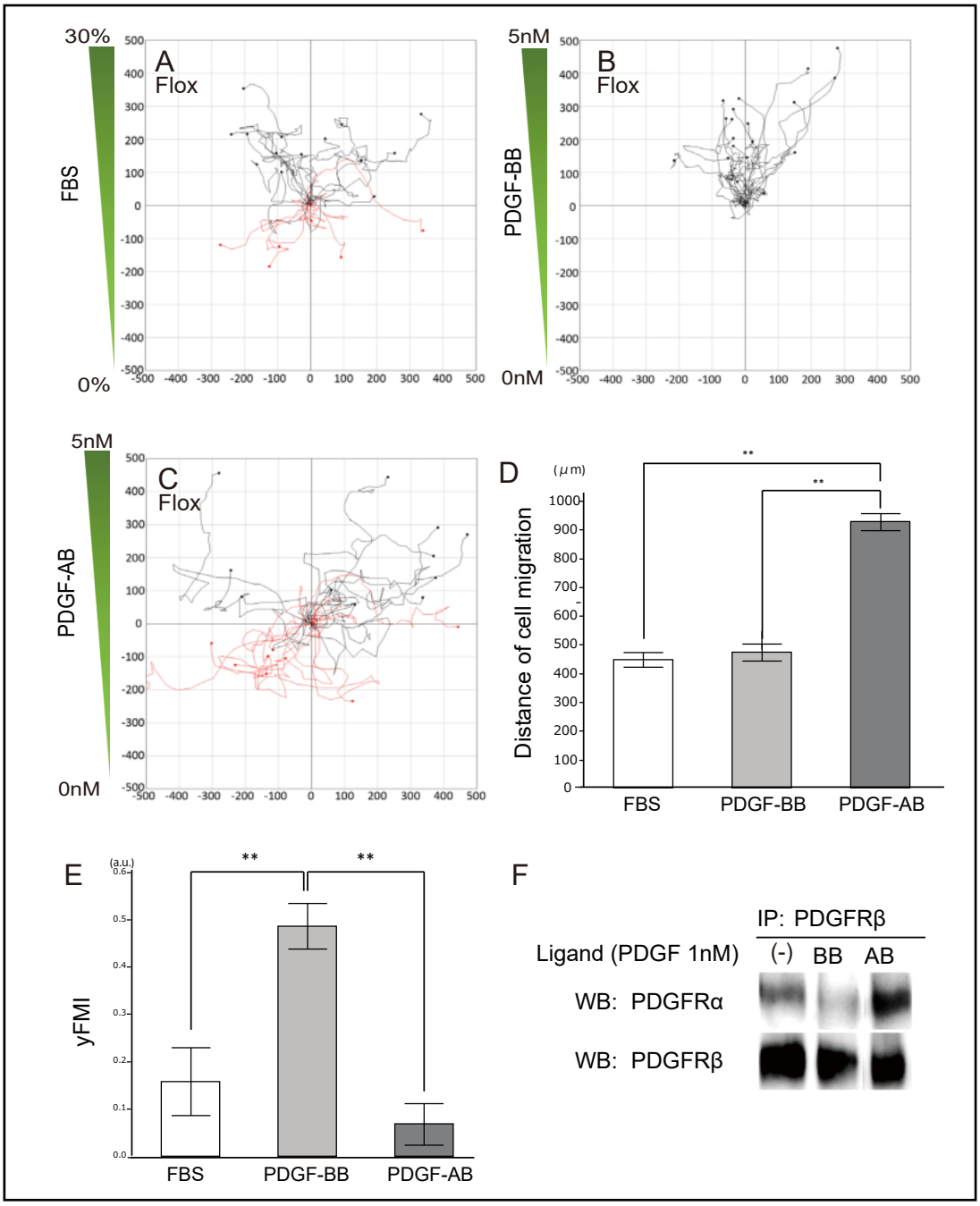

Fig. 2. Different chemoattractants induce random and directional migration in Flox fibroblasts. (A-C) Trajectories of Flox fibroblasts in response to an FBS gradient (30–0%) (A), PDGF-BB gradient (5–0 nM) (B), and PDGF-AB gradient (5–0 nM) (C). Black and red trajectory lines show, respectively, plus and minus net migration along the chemoattractant gradient. Green triangles indicate the chemoattractant gradient. (D and E) Distance of cell migration (D) and yFMI (E) of the Flox fibroblasts in the FBS gradient (30–0%), PDGF-BB gradient (5–0 nM), and PDGF-AB gradient (5–0 nM) over 24 h. Twenty cells were randomly selected from each experiment for preparing trajectories. Experiments were replicated a minimum of three times, and the representative results are presented. All error bars indicate the mean ± SEM. (** = $p<0.01$). (F) Immunoprecipitation using an anti-PDGFRβ antibody and immunoblotting using anti-PDGFRα or anti-PDGFRβ antibodies in Flox fibroblasts. Formation of PDGFRαβ heterodimers and PDGFRββ homodimers were induced after stimulation of Flox fibroblasts with 1 nM PDGF-AB or PDGF-BB for 10 min, respectively.

These data suggest that PDGFR*ββ* homodimers in α-KO fibroblasts are strong inducers of directionally persistent movement toward either FBS or PDGF-BB, while the effects of PDGFRαα are more subtle. Both PDGFR homodimers enhanced migration distance to a similar, small extent.

PDGFRαβ and PDGFRββ mediate random and directional migration, respectively, in Flox fibroblasts

Next, we examined the chemotaxis of control Flox fibroblasts expressing both PDGFRα and PDGFRβ subunits. In an FBS gradient of 30–0%, trajectories were complex, with frequent turns, and their net migrations were predominantly, but not exclusively, positive (Fig. 2A). In a PDGF-BB gradient of 5–0 nM, trajectories tended to orient towards the chemoattractant and also displayed positive net migration (Fig. 2B). Finally, the trajectories in a PDGF-AB gradient of 5–0 nM were highly diverse and complex, comprising both positive and negative net migrations (Fig. 2C). The migration distance was largest in the PDGF-AB gradient (Fig. 2D, distance, 451.12 ± 38.21 μm in FBS, 471.39 ± 29.67 μm in PDGF-BB, and 924.88 ± 29.58 μm in PDGF-AB, $p < 0.01$ in both FBS and PDGF-BB vs. PDGF-AB, respectively) but the yFMI was largest in the PDGF-BB gradient (Fig. 2E, yFMI, a.u., 0.15 ± 0.072 in FBS, 0.49 ± 0.048 in PDGF-BB, and 0.068 ± 0.044 in PDGF-AB, $p < 0.01$ in PDGF-BB vs. FBS and PDGF-BB vs. PDGF-AB). This suggests that the migration distance and directionality were differentially regulated in Flox fibroblasts by different chemoattractants.

Since different chemoattractants induced different mode of migration, we intended to examine the relationship between migration mode and PDGFR dimer type in Flox fibroblasts. In an immunoprecipitation assay, anti-PDGFRβ antibodies co-immunoprecipitated PDGFRα in Flox fibroblasts stimulated with PDGF-AB, but not in those stimulated with PDGF-BB (Fig. 2F). This PDGF-ligand dependency of different PDGFR dimer formation was further confirmed by use of HaloTag system (Supplementary Fig. 3). In accordance with previous reports, PDGF-AB and PDGF-BB appeared to preferentially induce PDGFRαβ and PDGFRββ, respectively, in Flox fibroblasts [22, 25]. Together with the fact that PDGFRββ in α-KO fibroblasts, but not PDGFRαα in β-KO fibroblasts, mediated chemotaxis with a high yFMI (Fig. 1E), it was concluded that directional and random migration of Flox fibroblasts (Fig. 2A–2C) was mediated by PDGFRββ in a PDGF-BB gradient and by PDGFRαβ in a PDGF-AB or FBS gradient, respectively.

High PDGF-BB gradients mediate directional migration in fibroblasts

Since mesenchymal cell proliferation and migration are mutually exclusive and PDGF at a high concentration (30 nM) did not induce NIH3T3 cell migration [37], the chemotaxis of Flox and α-KO fibroblasts in response to a high PDGF-BB gradient (50–0 nM) was examined. The net migration was mostly positive for both genotypes (Supplementary Fig. 4A and 4B). The migration distances were significantly greater in Flox fibroblasts and equivalent in α-KO fibroblasts when compared to the same genotype cultured with a low gradient (5–0 nM), as shown in Fig. 2B and Fig. 1F (Supplementary Fig. 4C, distance of Flox fibroblasts, 471.39 ± 29.67 μm in 5–0 nM vs. 938.90 ± 23.58 μm in 50–0 nM, $p < 0.01$; Supplementary Fig. 4E, distance of α-KO fibroblasts, 694.59 ± 36.68 μm in 5–0 nM vs. 641.69 ± 47.13 μm in 50–0 nM, differences were not significant). When compared to cells stimulated by the lower gradient, the yFMI of the Flox fibroblasts was equivalent and the yFMI of the α-KO fibroblasts was significantly decreased, while remaining at a significant level, as shown in Fig. 2B and Fig. 1F (Supplementary Fig. 4D, yFMI (a.u.) in Flox fibroblasts, 0.49 ± 0.05 in 5–0 nM vs. 0.42 ± 0.02 in 50–0 nM, difference was not significant; Supplementary Fig. 4F, yFMI (a.u.) in α-KO fibroblasts, 0.67 ± 0.03 in 5–0 nM PDGF-BB vs. 0.34 ± 0.059 in 50–0 nM PDGF-BB, $p < 0.01$). Thus, a high gradient of PDGF-BB increased the migration distance and preserved the high yFMI seen in Flox fibroblasts, while maintaining the migration distance of α-KO fibroblasts, despite a reduction in yFMI.

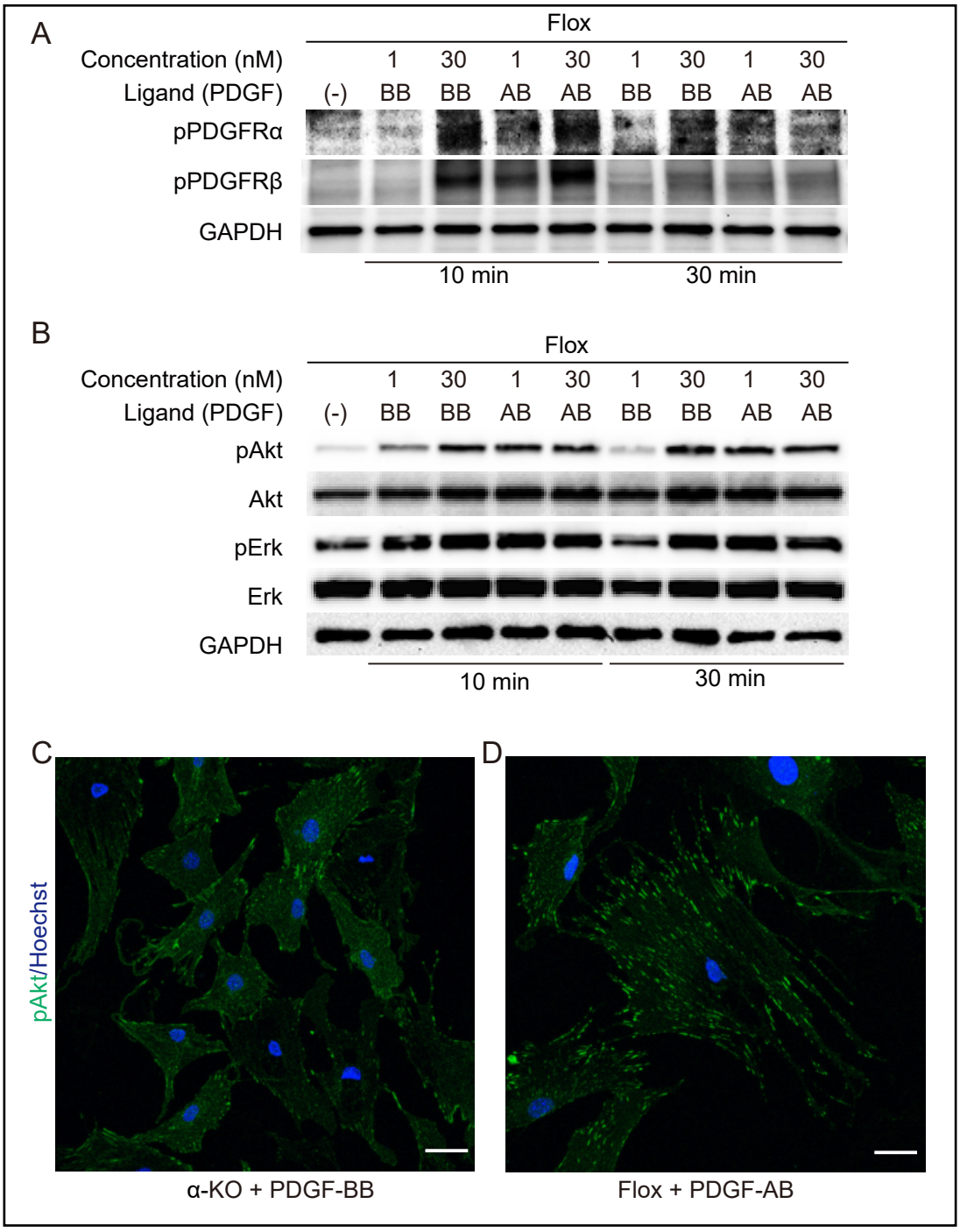

Fig. 3. PDGF-AB is a stronger activator of PDGFRs, Akt, and Erk than PDGF-BB. (A) Western blot analysis of the phosphorylated forms of PDGFRs (pPDGFRs), by use of phosphorylated PDGFR-specific antibodies, in Flox fibroblasts stimulated with 1 or 30 nM of PDGF-AB or PDGF-BB for 10 or 30 min. Equal protein loading was confirmed through the use of GAPDH as a housekeeping protein. (B) Western blot analysis of the phosphorylated forms of Akt (pAkt) and Erk (pErk) in Flox fibroblasts stimulated with 1 and 30 nM of PDGF-AB or PDGF-BB for 10 or 30 min. Equal protein loading was confirmed through the use of GAPDH as a housekeeping protein. (C and D) Immunofluorescent staining of pAkt (Green) in α-KO fibroblasts stimulated with 1 nM of PDGF-BB and Flox fibroblasts stimulated with 1 nM of PDGF-AB for 30 min within chamber slides that do not contain PDGF gradients. Nuclei were detected using Hoechst (blue). Scale bars = 50 μm. Experiments were replicated a minimum of three times, and the representative pictures are presented.

The Ras and PI3K pathways are necessary for random and directional migration, respectively

Activation of PDGFRs and their downstream signaling molecules was examined in order to determine the specific modes of migration mediated by PDGFRββ and PDGFRαβ in PDGF-BB and PDGF-AB gradients, respectively. Western blotting revealed that the phosphorylated forms of both PDGFRα and PDGFRβ that were undetectable in unstimulated condition turned detectable after the stimulation of either PDGF-BB and PDGF-AB in Flox fibroblasts (Fig. 3A, Supplementary Fig. 5A, B). Phosphorylated Akt (pAkt) in Flox fibroblasts were similarly high in response to 1 nM PDGF-AB and 30 nM of PDGF-AB and -BB but were relatively low in response to 1 nM of PDGF-BB (Fig. 3B, Supplementary Fig. 5C). pErk in Flox fibroblasts were relatively low in response to 1 nM of PDGF-BB at 30 min compared to other stimulated conditions (Fig. 3B, Supplementary Fig. 5D). Together with our immunoprecipitation results (Fig. 2F), these data showed that PDGFRαβ activated in Flox fibroblasts stimulated with PDGF-AB, is a more potent inducer of Akt and Erk activation than PDGFRββ activated in Flox fibroblasts stimulated with PDGF-BB, similar to previous reports [22, 25, 38]. In accordance with these data, the tiny dot-like accumulating foci of phosphorylated-Akt, corresponding to the adhesion points as confirmed by immunofluorescent stainings (Supplementary Fig. 6), were small in number and were mainly localized to the periphery of α-KO fibroblasts stimulated with PDGF-BB (Fig. 3C, Supplementary Fig. 7). In contrast, the spots of accumulated phosphorylated-Akt were many and were widely distributed in the cytoplasm of PDGF-AB-stimulated Flox fibroblasts (Fig. 3D, Supplementary Fig. 7). The level of Akt activation affected the distribution of activated Akt as well.

PI3K/Akt is one of the major downstream pathways of PDGFRs that drives cell movement [39]. Application of the PI3K inhibitor LY294002 totally deteriorated the directional migration of α-KO fibroblasts exposed to a PDGF-BB gradient, when compared to that obtained under similar conditions but without inhibitor, as shown in Fig. 1F (Fig. 4A and 4C, yFMI a.u., −0.076 ± 0.038 with LY294002 vs. 0.69 ± 0.031 without LY294002, $p < 0.01$). In contrast, LY294002 did not affect the migration distance (Fig. 4A and 4B, distance, 783.16 ± 55.19μm with LY294002, 694.59 ± 36.68 μm without LY294002, difference is not significant). Similarly, PI3K inhibitor significantly suppressed directionality (Fig. 4D and F, yFMI a.u., 0.18 ± 0.053 with LY294002 vs. 0.49 ± 0.048 without LY294002, $p < 0.01$) and suppressed migration distance to lesser extents (Fig. 4D and 4E, distance, 371.49 ± 33.02 μm with LY294002 vs. 471.39 ± 29.67 μm without LY294002, $p < 0.05$) in Flox fibroblasts exposed to a PDGF-BB gradient as compared with those obtained in the same conditions but without inhibitor treatment, as shown in Fig. 2B. PI3K activation was definitely necessary for the directionality but not for the distance in PDGFRββ-mediated directional migration.

The role of Ras/MAP kinase in the PDGFRαβ-mediated random migration of Flox fibroblasts was examined, since PDGFRαβ has been shown to be a more potent activator of Ras/MAP kinase than PDGFR homodimers in both the present study (Fig. 3B, Supplementary Fig. 5) and in previous reports [22, 25, 38]. MEK inhibitor (PD98059, Fig. 4G) and Ras inhibitor (farnesyl thiosalicylic acid, FTA, Fig. 4H) similarly suppressed the migration distance of Flox fibroblasts exposed to a PDGF-AB gradient when compared to previous experiments without inhibitors, as shown in Fig. 2C (Fig. 4I, distance, 523.27 ± 37.31 μm with PD98059, 442.77 ± 17.01 μm with FTA, 924.88 ± 29.58 μm without inhibitors, $p < 0.01$ when comparing PD98059 or FTA-treated samples to untreated samples). On the other hand, FTA (Fig. 4H), but not PD98059, (Fig. 4G), significantly increased yFMI in the same experimental conditions (Fig. 4J, yFMI a.u., 0.11 ± 0.08 with PD98059, 0.36 ± 0.05 with FTA; 0.068 ± 0.044 without inhibitor, $p < 0.01$ when comparing FTA treatment with PD98059 or untreated cells). Both Ras and MEK increased the migration distance and Ras, but not MEK, mediated random migration downstream of activated PDGFRαβ, indicating that Ras signaling pathways other than Ras/MEK/MAP kinases are necessary to mediate random migration.

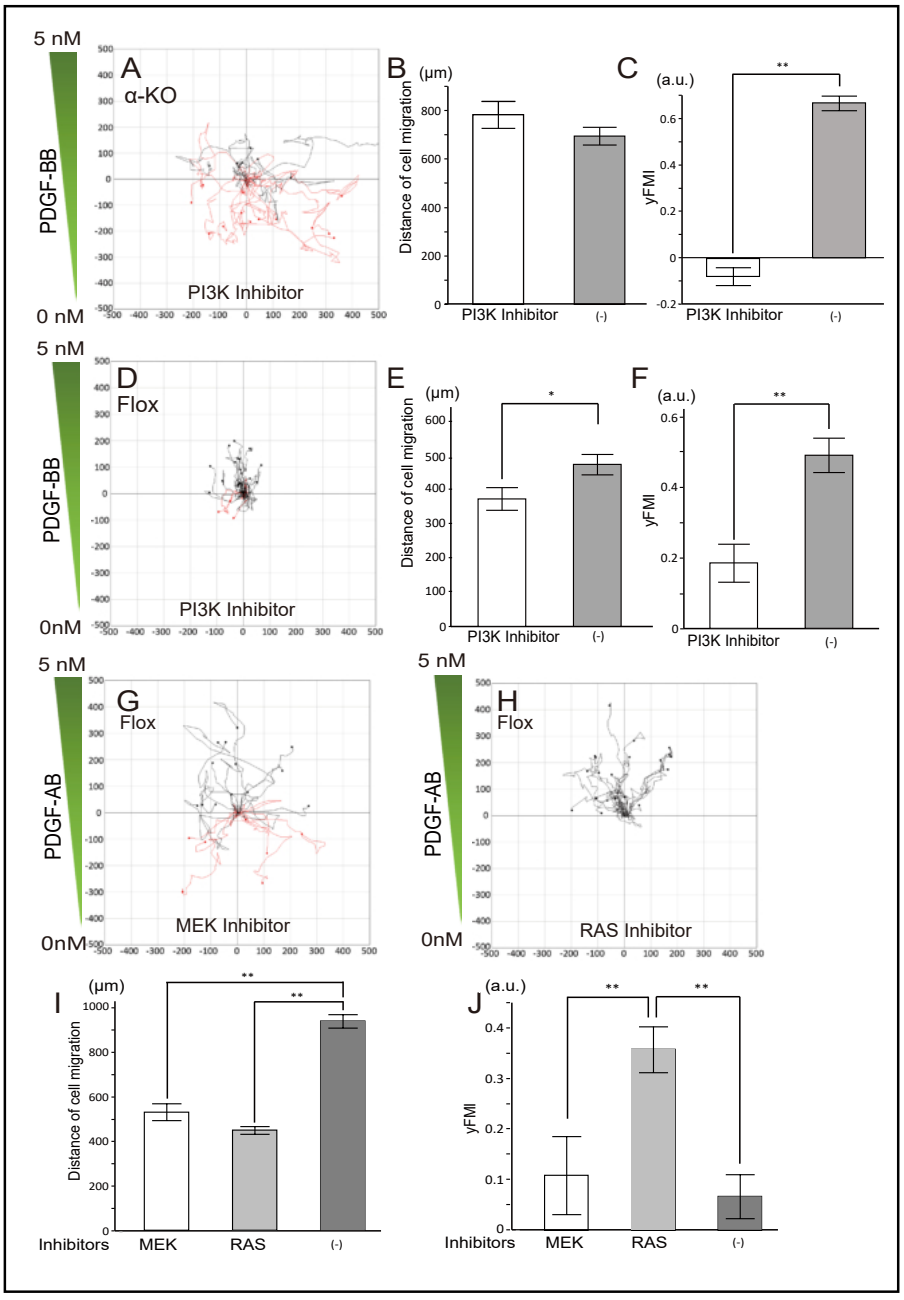

Fig. 4. PI3K and Ras are necessary for directional and random migration, respectively. (A) The trajectory of α-KO fibroblasts treated with PI3K inhibitor LY294002. (B and C) The distance of cell migration (B) and yFMI (C) of α-KO fibroblasts treated with PI3K inhibitor, as compared to the untreated cells seen in Fig. 1F. (D) The trajectory of Flox fibroblasts treated with PI3K inhibitor. (E and F) The distance of cell migration (E) and yFMI (F) of Flox fibroblasts treated with PI3K inhibitor, as compared with the untreated cells seen in Fig. 2B. (G and H) The trajectory of Flox fibroblasts treated with MEK inhibitor PD98059 (G) and RAS inhibitor FTA (H). (I and J) The distance of cell migration (I) and yFMI (J) of Flox fibroblasts exposed to a PDGF-AB gradient (5–0 nM) over 24 h and treated with MEK inhibitor PD98059, Ras inhibitor FTA, or without inhibitors, as determined in Fig. 2C. Black and red trajectory lines show plus and minus net migration along the chemoattractant gradient, respectively. Green triangles indicate the gradient of chemoattractant. Twenty cells were randomly selected from each experiment for preparing trajectories. Experiments were replicated a minimum of three times, and the representative results are presented. All error bars indicate the mean ± SEM. (* = $p<0.05$, ** = $p<0.01$).

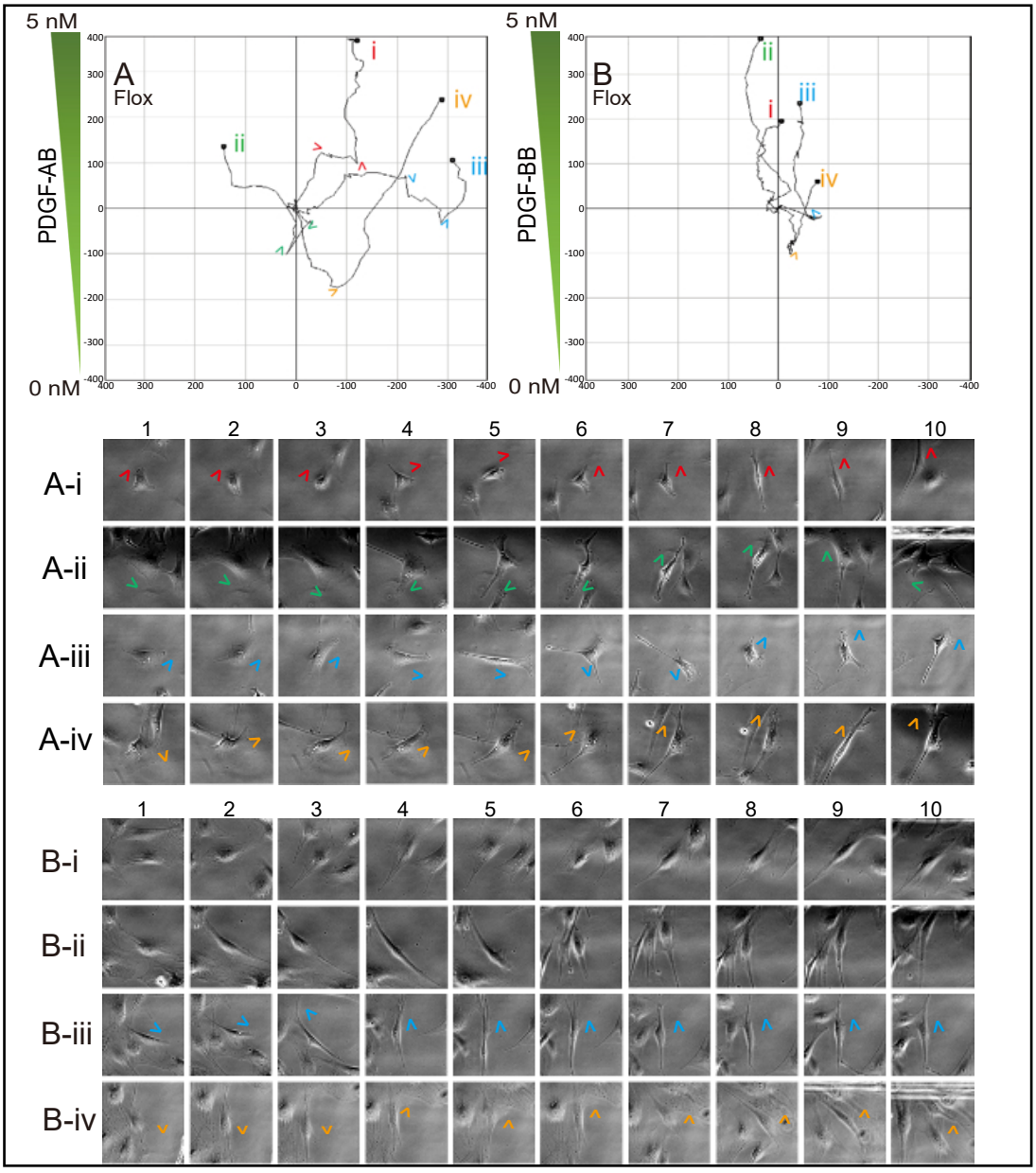

Fig. 5. Changes in cell shape are associated with frequent turning during random migration. (A and B) The trajectories of Flox fibroblasts stimulated by PDGF-AB or PDGF-BB. (A) The trajectories of four randomly selected Flox fibroblasts stimulated with a PDGF-AB gradient (5–0 nM). (B) The trajectories of four selected α-KO fibroblasts stimulated with a PDGF-BB gradient (5–0 nM), including those with typical directional migration that does not display large-scale turning (B-i and B-ii) as well as those with exceptionally large turning angles (B-iii and B-iv). Arrowheads indicate new directions after turning at a large angle. (A-i–iv and B-i-iv) Phase contrast images prepared from a time lapse video monitoring the four cells shown in (A) and (B). Representative images from each cell were isolated and arranged from left to right to demonstrate the sequential changes in cell morphology over time. The large angle turns indicated by arrowheads in the trajectories correspond to the A-i4 and A-i6 images from A-i trajectories; A-ii4 and A-ii7 from A-ii ; A-iii6 and A-iii8 from A-iii; A-iv2 from A-iv; B-iii3 from B-iii; B-iv4 from B-iv, respectively. Branch-like cytoplasmic protrusions were generated toward the new direction after large scale, high frequency turning in random migration (A-i-iv) except for in A-ii7. Cell shapes were consistent in directional migration (B). Large angle turning was carried out by turning back without changing the long axis of spindle-shaped cells (A-ii7, B-iii3, and B-iv4).

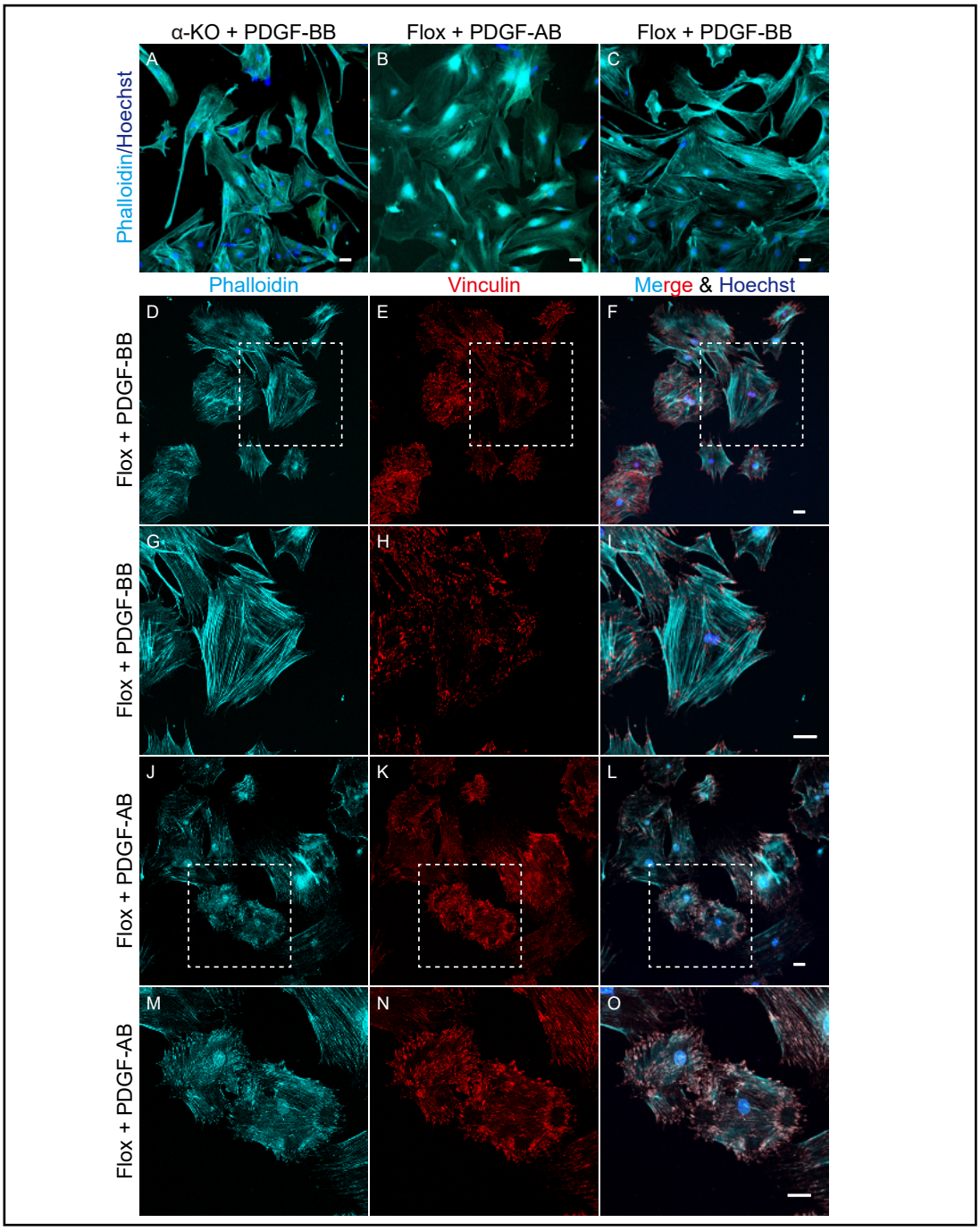

Fig. 6. PDGF-BB and PDGF-AB differentially regulate cytoskeletal remodeling. (A–C) F-actin staining (cyan) by phalloidin of migrating fibroblasts in a μ-migration chamber. Ventral stress fibers are distinct in spindle-shaped α-KO fibroblasts (A) and Flox fibroblasts (C) under a PDGF-BB gradient (5–0 nM), but were obscure in Flox fibroblasts (B) under a PDGF-AB gradient (5–0 nM) following 20 h of migration. (D–O) Phalloidin staining of F-actin (cyan) and vinculin staining of adhesion points (red). (D–I). Flox fibroblasts cultured for 24h in 5 nM PDGF-BB without a gradient (D–F) and magnified view of dotted areas in D–F (G–I). Stress fibers are distinct and long and are arranged in parallel, connecting vinculin-positive adhesion points at both ends of cells (F, I). (J–O) Flox fibroblasts cultured for 24h in 5 nM PDGF-AB without a gradient (J–L) and magnified view of dotted areas in J–L (M–O). Stress fibers are thin and short, and are arranged in random directions connecting vinculin positive adhesion points. Nuclei were imaged using Hoechst (blue). Scale bars indicate 50 μm.

The cytomorphology of fibroblasts varies in accordance with migration mode

Changes in cell shape and cytoskeletal remodeling were examined through time-lapse video monitoring of cell migration. During the processes of random migration in Flox fibroblasts, each large angle turn was associated with changes in cell shape; cytoplasmic protrusions, like branches, were oriented towards the new direction and grew up at the lateral part of cytoplasm, where they comprised the nascent leading edge (Fig. 5A, 5Ai–iv and Supplementary Video 1) as previously reported [40]. In the directionally-persistent migration of α-KO fibroblasts, cell shape also tended to persist; these cells often had a narrow, spindle-shaped cytoplasm with a leading edge headed towards increased PDGF-BB concentration and branch-like protrusions were far less frequent than in random migration (Fig. 5B, 5Bi–iv and Supplementary Video 2). It was of note that, in directional migration, large angle turns were less frequent and, when present, were processed by turning back while keeping the cell's major longitudinal axis of spindle-shaped cytoplasm in a similar orientation, and not by branching or nascent process formations (Fig. 5B–iii and 5B–iv).

Ventral and dorsal stress fibers, as well as transverse arcs, are F-actins. Only ventral stress fibers connect two adhesion points and contribute to establish a front-to-rear axis of migrating cells [41]. α-KO fibroblasts migrating within a PDGF-BB gradient tended to be spindle shaped and were abundant in ventral stress fibers that often spanned the entire length of the cellular axis (Fig. 6A). These fibers were obscured in Flox fibroblasts migrating through a PDGF-AB gradient (Fig. 6B) and were again distinctive in Flox fibroblasts when exposed to a PDGF-BB gradient (Fig. 6C). Because the structure of the μ-migration chamber is not suited for the multiple steps of immunostaining, actin and adhesion points of Flox fibroblasts were stained in a standard chamber slide with PDGF-containing medium but without a concentration gradient. In the presence of PDGF-BB, conspicuous ventral stress fibers arranged in parallel showed fascicular configuration, and frequently connected two vinculin-positive adhesion points that were localized at opposite poles of the cell (Fig. 6D–6I). When exposed to PDGF-AB, ventral stress fibers were relatively obscure compared with those from the PDGF-BB treatment, and were short, with intricate arrangements connecting many vinculin-positive adhesions distributed widely in the cytoplasm (Fig. 6J–6O, Supplementary Fig. 8). Therefore, the formation of conspicuous ventral stress fibers was a feature of α-KO and Flox fibroblasts with induced PDGFRββ, but not with PDGFRαβ, and was commonly seen in samples treated both with and without chemotactic gradients.

PDGFRαβand PDGFRββ similarly mediate the healing of in vitro scratch wounds

Finally, the contributions of different PDGFR dimers were examined using a scratch wound healing assay, which is another method used to analyze cell migration *in vitro*. Wound closure was significantly enhanced to the similar extents by PDGFRαβ and PDGFRββ in Flox and α-KO fibroblasts, respectively, in 10% FBS containing D-MEM, in comparison to control αβ-KO fibroblasts (Fig. 7A and 7B; $p < 0.01$ vs. Flox and vs. α-KO). Wound closure was significantly suppressed by PDGFRαα in β-KO when compared to similarly-treated αβ-KO control fibroblasts (Fig. 7A and 7B; $p < 0.05$, vs. αβ-KO). These results were compatible with our previous report showing that the migration of fibroblasts into the scratched wound depends on the PDGFRβ, but not PDGFRα, subunit in the same experimental models [26].

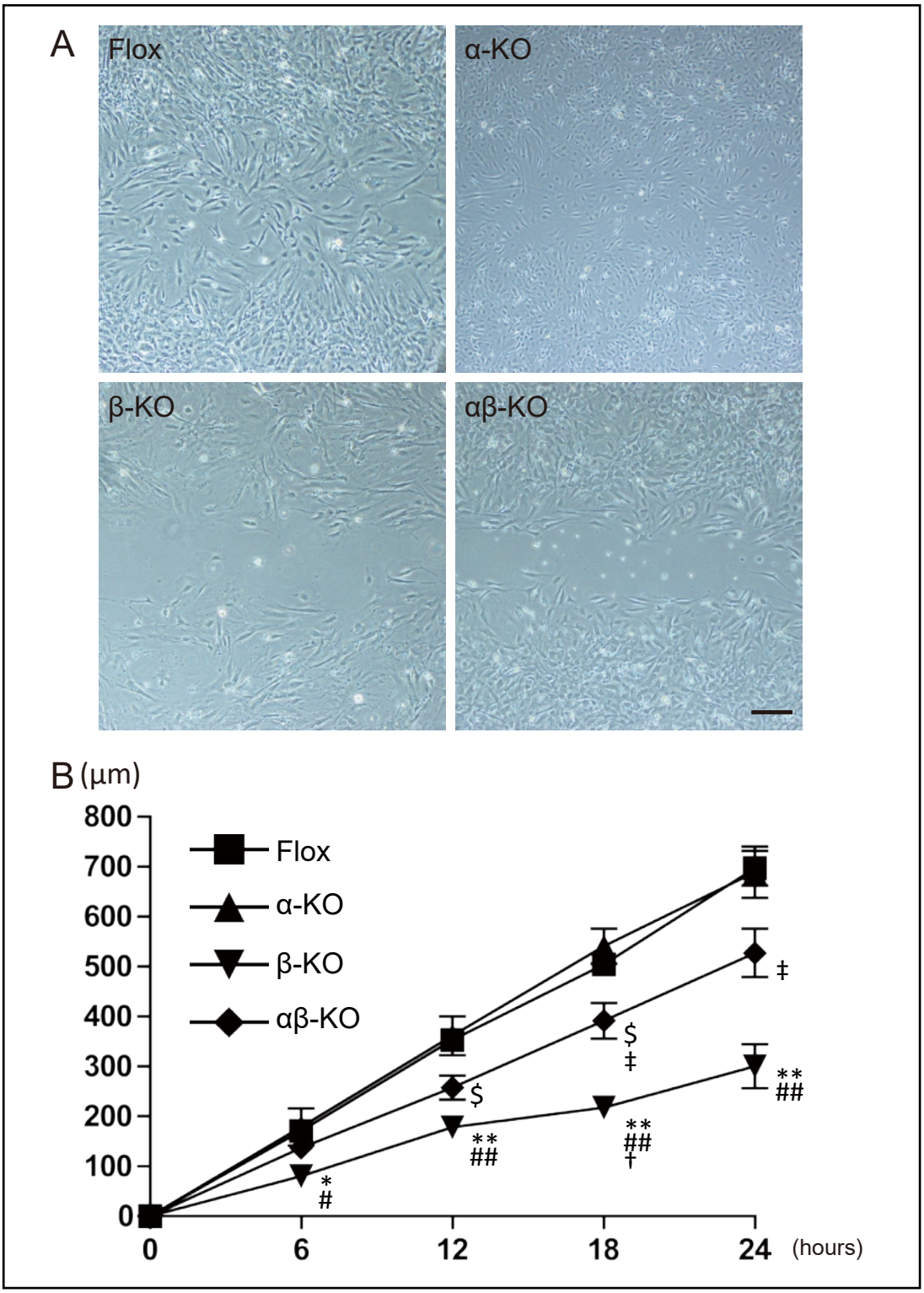

Fig. 7. Wound scratch assay on conditional *Pdgfr* knockout fibroblasts. (A) Phase contrast images showing an overview of *Pdgfr* knockout fibroblasts at 24 h after scratch injury in vitro. (B) Line graph showing the wound closure rates of *Pdgfr* knockout fibroblasts. Significant differences are indicated as follows: * = p<0.05 and ** = p<0.01 for α-KO vs. β-KO; # = p<0.05 and ## = p<0.01 for Flox vs. β-KO; $ = p<0.05 for Flox vs. α/β-KO; † = p<0.05 and †† = p<0.01 for α/β-KO vs. β-KO, and ‡ = p<0.05 for α-KO vs. α/β-KO. n = 3–5. Scale bar indicates 300 m. Experiments were replicated three times, and the representative results are presented.

Discussion

Whereas the molecular mechanisms of random cell migration have been characterized, no one mechanism has been revealed that can integrate cell signaling with the mediation of directionally persistent migration in mesenchymal cells. In the present study, through the combination of different PDGF ligand stimulations and *Pdgfr* gene knockout cells, we found that PDGFRββ and PDGFRαβ dimers were potent mediators of directionally-persistent and random migrations, respectively, in primary cultured mouse skin fibroblasts. Beside these, PDGFRαβ accelerated the velocity of cell movement, whereas the effects of PDGFRββ on the velocity were subtle. These PDGFR dimer-specific roles were found in *Pdgfr* gene knockout cells, and were also confirmed in control Flox fibroblasts through the use of different PDGF ligand and serum stimulations. PDGFRαα also mediated directional migration with low directionality and did not accelerate migration velocity. Accordingly, it was clear that the directional versus random migration of fibroblasts is differentially defined by the PDGFR dimer subtype. It is of note that these dimer subtype-specific phenomena are anticipated to occur *in vivo*, since these phenomena were reproduced in the control fibroblasts expressing both PDGFRs, depending on the choice of different ligands.

In our study, PI3K and Ras, two major mediators of receptor phospho-tyrosine kinase chemotactic input [39, 42, 43], differentially mediate directional and random migrations, respectively. We showed that PI3K inhibitor mediated the robust transition from directional to random migration in PDGFRα-KO fibroblasts stimulated with a PDGF-BB gradient, without affecting migration distance. Activated Akt was mainly localized in the periphery of α-KO fibroblasts exposed to PDGF-BB, while it was widely distributed in the cytoplasm of control Flox fibroblasts exposed to PDGF-AB. Similarly to these, PI3K/Akt signaling accumulated in the protruding lamellipodia at the leading edge of migrating fibroblasts in a previous live imaging study [13]. In this study, Melvin and colleagues determined that PI3K/Akt signaling mediated the maturation of selected protrusions out of the randomly formed and unstable protrusions induced by Rac1, into actin rich protrusions or lamellipodia that comprised a stabilized leading edge to maintain directional migration during a relatively long range of 20–70 min [40, 44, 45]. Accordingly, it was hypothesized that PI3K signaling stabilized the protruding end of fibroblasts at the leading edge and mediated directionally-persistent migration in α-KO fibroblasts.

In the present study, the PDGFRαβ heterodimer induced more potent activation of Erk and Akt than the PDGFRββ homodimer. Furthermore, Ras inhibitor, but not MEK inhibitor, significantly increased the directionality and suppressed the velocity of randomly migrating Flox fibroblasts. Similarly, previous studies have shown that the PDGFRαβ heterodimer is a stronger activator of Ras/MAP kinase pathway than PDGFR homodimers [38]. Moreover, hyperactivation of Ras, but not Raf, caused directional defects in the motility of NIH3T3 fibroblasts toward PDGF in a Boyden chamber assay [46]. Altogether, our study indicates that Ras plays a role in mediating random migration with high velocity in Flox fibroblasts and that the induction of either directional or random movement in fibroblasts could depend on the signaling features specific to each PDGFR dimer.

Prominent ventral stress fibers connecting the attaching points localized at opposite poles of the cells were characteristics of PDGF-BB-stimulated α-KO and control Flox fibroblasts both with and without PDGF-BB gradient. Rho family GTPases are activated by PDGF and crucially reorganize cytoskeletons and cell adhesion [7, 9]. Among them, Rho A contributes to maintain the front-to-rear polarity by mediating ventral stress fiber formation [47] and by suppressing Rac1 mediated generation of random lateral protrusions [10, 11]. These findings support the notion that the prominent ventral stress fiber formation may contribute to the directionally-persistent migration mediated by PDGFRββ in the present study. Besides that, Ras was a mediator of random migration in both ours and a previous study [46]. It is of note that this effect of Ras was not dependent on the Ras/Raf/MEK/MAPK pathway in either study, since neither MEK nor Raf was involved in the directional migration of fibroblasts in ours or a previous study [46]. Other divergent pathways like Ras/Rac1

need to be considered as effectors for Ras-mediated random migration because Rac1 is a downstream mediator of Ras that induces random migration [48-50]. After all, different Rho GTPases may act as downstream mediators of PDGFR dimer-specific modes of migration in fibroblasts, though further direct evidence is needed in order to explore these correlations.

Both α-KO and Flox fibroblasts had accelerated wound healing *in vitro* when compared to αβ-KO fibroblasts, similar to our previous study [26]. It may be indicated that both directional and random migrations could contribute to *in vivo* wound healing. Separately, differential roles for each mode of migration may be required, e.g., most typically the vascular endothelial cell-derived PDGF-BB may be used to mediate directional migration via PDGFRββ activation for the precise recruitment of pericytes during angiogenesis and vasculogenesis [20, 33, 51], and the PDGF-AB and PDGF-CC released from platelets may induce random migration via PDGFRαβ activation and allow recruited fibroblasts to explore the tissue defects of injured sites [19, 22-25]. The functional relevance of each mode of cellular motility deserves further study, depending on each pathophysiological condition.

Compared to the high velocity and high directionality of leukocyte migration, mesenchymal cell migration is slow and directionality has long been considered obscure. However, in the present study, for the first time, we have demonstrated that directional and random migration can be tightly regulated for up to 24 h in fibroblasts exposed to a soluble chemotactic cue depending on PDGFR dimer subtype. These strategies may be responsible for the efficient recruitment of mesenchymal cells, including fibroblasts, throughout our bodies on demand. Further studies are required to understand the regulatory mechanisms of mesenchymal cell motility collectively.

Acknowledgements

We thank members of the Department of Pathology and Life Science Research Center at the University of Toyama for thoughtful discussions and careful animal care. This work was supported by JSPS KAKENHI Grant Numbers JP25293093/JP17H04062 (to M. S.), JP15K08396 (to Y. I.), and JP26460360 (to S. Y.). K. Y., Y. I. and S. Y. conceived and designed the project. K. Y., T. H., Y. I., S. Y., N. O., N. Y., M. Y., T. T. H., N. S., K. T., T. F. and H. M. performed experiments. K. Y., Y. I. and S. Y. wrote the manuscript with significant input from K. F., M. N. and M. S..

Disclosure Statement

The authors declare no competing financial interests.

References

1 Petrie RJ, Doyle AD, Yamada KM: Random versus directionally persistent cell migration. Nat Rev Mol Cell Biol 2009;10:538-549.
2 Swaney KF, Huang CH, Devreotes PN: Eukaryotic chemotaxis: a network of signaling pathways controls motility, directional sensing, and polarity. Annu Rev Biophys 2010;39:265-289.
3 Vorotnikov AV: Chemotaxis: movement, direction, control. Biochemistry (Mosc) 2011;76:1528-1555.
4 Bear JE, Haugh JM: Directed migration of mesenchymal cells: where signaling and the cytoskeleton meet. Curr Opin Cell Biol 2014;30:74-82.
5 Friedl P, Wolf K: Plasticity of cell migration: a multiscale tuning model. J Cell Biol 2010;188:11-19.
6 Vicente-Manzanares M, Zareno J, Whitmore L, Choi CK, Horwitz AF: Regulation of protrusion, adhesion dynamics, and polarity by myosins IIA and IIB in migrating cells. J Cell Biol 2007;176:573-580.
7 Goicoechea SM, Awadia S, Garcia-Mata R: I'm coming to GEF you: Regulation of RhoGEFs during cell migration. Cell Adh Migr 2014;8:535-549.

8 Guilluy C, Garcia-Mata R, Burridge K: Rho protein crosstalk: another social network? Trends Cell Biol 2011;21:718-726.
9 Jimenez C, Portela RA, Mellado M, Rodriguez-Frade JM, Collard J, Serrano A, Martinez AC, Avila J, Carrera AC: Role of the PI3K regulatory subunit in the control of actin organization and cell migration. J Cell Biol 2000;151:249-262.
10 Vega FM, Fruhwirth G, Ng T, Ridley AJ: RhoA and RhoC have distinct roles in migration and invasion by acting through different targets. J Cell Biol 2011;193:655-665.
11 Worthylake RA, Burridge K: RhoA and ROCK promote migration by limiting membrane protrusions. J Biol Chem 2003;278:13578-13584.
12 Kundra V, Escobedo JA, Kazlauskas A, Kim HK, Rhee SG, Williams LT, Zetter BR: Regulation of chemotaxis by the platelet-derived growth factor receptor-beta. Nature 1994;367:474-476.
13 Melvin AT, Welf ES, Wang Y, Irvine DJ, Haugh JM: In chemotaxing fibroblasts, both high-fidelity and weakly biased cell movements track the localization of PI3K signaling. Biophys J 2011;100:1893-1901.
14 Monypenny J, Zicha D, Higashida C, Oceguera-Yanez F, Narumiya S, Watanabe N: Cdc42 and Rac family GTPases regulate mode and speed but not direction of primary fibroblast migration during platelet-derived growth factor-dependent chemotaxis. Mol Cell Biol 2009;29:2730-2747.
15 Pankov R, Endo Y, Even-Ram S, Araki M, Clark K, Cukierman E, Matsumoto K, Yamada KM: A Rac switch regulates random versus directionally persistent cell migration. J Cell Biol 2005;170:793-802.
16 Dang I, Gorelik R, Sousa-Blin C, Derivery E, Guerin C, Linkner J, Nemethova M, Dumortier JG, Giger FA, Chipysheva TA, Ermilova VD, Vacher S, Campanacci V, Herrada I, Planson AG, Fetics S, Henriot V, David V, Oguievetskaia K, Lakisic G et al.: Inhibitory signalling to the Arp2/3 complex steers cell migration. Nature 2013;503:281-284.
17 Castellano E, Molina-Arcas M, Krygowska AA, East P, Warne P, Nicol A, Downward J: RAS signalling through PI3-Kinase controls cell migration via modulation of Reelin expression. Nat Commun 2016;7:11245.
18 Deuel TF, Kawahara RS, Mustoe TA, Pierce AF: Growth factors and wound healing: platelet-derived growth factor as a model cytokine. Annu Rev Med 1991;42:567-584.
19 Singer AJ, Clark RA: Cutaneous wound healing. N Engl J Med 1999;341:738-746.
20 Andrae J, Gallini R, Betsholtz C: Role of platelet-derived growth factors in physiology and medicine. Genes Dev 2008;22:1276-1312.
21 Shim AH, Liu H, Focia PJ, Chen X, Lin PC, He X: Structures of a platelet-derived growth factor/propeptide complex and a platelet-derived growth factor/receptor complex. Proc Natl Acad Sci U S A 2010;107:11307-11312.
22 Ekman S, Kallin A, Engstrom U, Heldin CH, Ronnstrand L: SHP-2 is involved in heterodimer specific loss of phosphorylation of Tyr771 in the PDGF beta-receptor. Oncogene 2002;21:1870-1875.
23 Fang L, Yan Y, Komuves LG, Yonkovich S, Sullivan CM, Stringer B, Galbraith S, Lokker NA, Hwang SS, Nurden P, Phillips DR, Giese NA: PDGF C is a selective alpha platelet-derived growth factor receptor agonist that is highly expressed in platelet alpha granules and vascular smooth muscle. Arterioscler Thromb Vasc Biol 2004;24:787-792.
24 Hart CE, Bailey M, Curtis DA, Osborn S, Raines E, Ross R, Forstrom JW: Purification of PDGF-AB and PDGF-BB from human platelet extracts and identification of all three PDGF dimers in human platelets. Biochemistry 1990;29:166-172.
25 Rupp E, Siegbahn A, Ronnstrand L, Wernstedt C, Claesson-Welsh L, Heldin CH: A unique autophosphorylation site in the platelet-derived growth factor alpha receptor from a heterodimeric receptor complex. Eur J Biochem 1994;225:29-41.
26 Gao Z, Sasaoka T, Fujimori T, Oya T, Ishii Y, Sabit H, Kawaguchi M, Kurotaki Y, Naito M, Wada T, Ishizawa S, Kobayashi M, Nabeshima Y, Sasahara M: Deletion of the PDGFR-beta gene affects key fibroblast functions important for wound healing. J Biol Chem 2005;280:9375-9389.
27 Koyama N, Hart CE, Clowes AW: Different functions of the platelet-derived growth factor-alpha and -beta receptors for the migration and proliferation of cultured baboon smooth muscle cells. Circ Res 1994;75:682-691.
28 Nister M, Hammacher A, Mellstrom K, Siegbahn A, Ronnstrand L, Westermark B, Heldin CH: A glioma-derived PDGF A chain homodimer has different functional activities from a PDGF AB heterodimer purified from human platelets. Cell 1988;52:791-799.

29 Clement DL, Mally S, Stock C, Lethan M, Satir P, Schwab A, Pedersen SF, Christensen ST: PDGFRalpha signaling in the primary cilium regulates NHE1-dependent fibroblast migration via coordinated differential activity of MEK1/2-ERK1/2-p90RSK and AKT signaling pathways. J Cell Sci 2013;126:953-965.
30 Horikawa S, Ishii Y, Hamashima T, Yamamoto S, Mori H, Fujimori T, Shen J, Inoue R, Nishizono H, Itoh H, Majima M, Abraham D, Miyawaki T, Sasahara M: PDGFRalpha plays a crucial role in connective tissue remodeling. Sci Rep 2015;5:17948.
31 Hayashi S, McMahon AP: Efficient recombination in diverse tissues by a tamoxifen-inducible form of Cre: a tool for temporally regulated gene activation/inactivation in the mouse. Dev Biol 2002;244:305-318.
32 Lee J, Veatch SL, Baird B, Holowka D: Molecular mechanisms of spontaneous and directed mast cell motility. J Leukoc Biol 2012;92:1029-1041.
33 Shen J, Ishii Y, Xu G, Dang TC, Hamashima T, Matsushima T, Yamamoto S, Hattori Y, Takatsuru Y, Nabekura J, Sasahara M: PDGFR-beta as a positive regulator of tissue repair in a mouse model of focal cerebral ischemia. J Cereb Blood Flow Metab 2012;32:353-367.
34 Yamamoto S, Yoshino I, Shimazaki T, Murohashi M, Hevner RF, Lax I, Okano H, Shibuya M, Schlessinger J, Gotoh N: Essential role of Shp2-binding sites on FRS2alpha for corticogenesis and for FGF2-dependent proliferation of neural progenitor cells. Proc Natl Acad Sci U S A 2005;102:15983-15988.
35 Sato H, Ishii Y, Yamamoto S, Azuma E, Takahashi Y, Hamashima T, Umezawa A, Mori H, Kuroda S, Endo S, Sasahara M: PDGFR-beta Plays a Key Role in the Ectopic Migration of Neuroblasts in Cerebral Stroke. Stem Cells 2016;34:685-698.
36 Yamamoto S, Muramatsu M, Azuma E, Ikutani M, Nagai Y, Sagara H, Koo BN, Kita S, O'Donnell E, Osawa T, Takahashi H, Takano KI, Dohmoto M, Sugimori M, Usui I, Watanabe Y, Hatakeyama N, Iwamoto T, Komuro I, Takatsu K: A subset of cerebrovascular pericytes originates from mature macrophages in the very early phase of vascular development in CNS. Sci Rep 2017;7:3855.
37 De Donatis A, Comito G, Buricchi F, Vinci MC, Parenti A, Caselli A, Camici G, Manao G, Ramponi G, Cirri P: Proliferation versus migration in platelet-derived growth factor signaling: the key role of endocytosis. J Biol Chem 2008;283:19948-19956.
38 Ekman S, Thuresson ER, Heldin CH, Ronnstrand L: Increased mitogenicity of an alphabeta heterodimeric PDGF receptor complex correlates with lack of RasGAP binding. Oncogene 1999;18:2481-2488.
39 Manning BD, Cantley LC: AKT/PKB signaling: navigating downstream. Cell 2007;129:1261-1274.
40 Welf ES, Ahmed S, Johnson HE, Melvin AT, Haugh JM: Migrating fibroblasts reorient directionality by a metastable, PI3K-dependent mechanism. J Cell Biol 2012;197:105-114.
41 Kassianidou E, Kumar S: A biomechanical perspective on stress fiber structure and function. Biochim Biophys Acta 2015;1853:3065-3074.
42 Charest PG, Firtel RA: Big roles for small GTPases in the control of directed cell movement. Biochem J 2007;401:377-390.
43 Kolsch V, Charest PG, Firtel RA: The regulation of cell motility and chemotaxis by phospholipid signaling. J Cell Sci 2008;121:551-559.
44 Andrew N, Insall RH: Chemotaxis in shallow gradients is mediated independently of PtdIns 3-kinase by biased choices between random protrusions. Nat Cell Biol 2007;9:193-200.
45 Arrieumerlou C, Meyer T: A local coupling model and compass parameter for eukaryotic chemotaxis. Dev Cell 2005;8:215-227.
46 Kundra V, Anand-Apte B, Feig LA, Zetter BR: The chemotactic response to PDGF-BB: evidence of a role for Ras. J Cell Biol 1995;130:725-731.
47 Vallenius T: Actin stress fibre subtypes in mesenchymal-migrating cells. Open Biol 2013;3:130001.
48 Gardel ML, Schneider IC, Aratyn-Schaus Y, Waterman CM: Mechanical integration of actin and adhesion dynamics in cell migration. Annu Rev Cell Dev Biol 2010;26:315-333.
49 Innocenti M, Tenca P, Frittoli E, Faretta M, Tocchetti A, Di Fiore PP, Scita G: Mechanisms through which Sos-1 coordinates the activation of Ras and Rac. J Cell Biol 2002;156:125-136.
50 Wu YI, Frey D, Lungu OI, Jaehrig A, Schlichting I, Kuhlman B, Hahn KM: A genetically encoded photoactivatable Rac controls the motility of living cells. Nature 2009;461:104-108.
51 Armulik A, Genove G, Mae M, Nisancioglu MH, Wallgard E, Niaudet C, He L, Norlin J, Lindblom P, Strittmatter K, Johansson BR, Betsholtz C: Pericytes regulate the blood-brain barrier. Nature 2010;468:557-561.